



RESEARCH ARTICLE

# Pectin micro-encapsulation of pretilachlor for smart herbicide delivery through biopolymer guided slow release

S Vignesh<sup>1\*</sup>, P Murali Arthanari<sup>1</sup>, R Kalpana<sup>1</sup>, P Janaki<sup>2</sup>, S Karthikeyan<sup>3</sup> & R Umarani<sup>4</sup>

<sup>1</sup>Department of Agronomy, Tamil Nadu Agricultural University, Coimbatore 641 003, Tamil Nadu, India

<sup>2</sup>Department of Soil Science and Agricultural Chemistry, Tamil Nadu Agricultural University, Coimbatore 641 003, Tamil Nadu, India

<sup>3</sup>Department of Agricultural Microbiology, Tamil Nadu Agricultural University, Coimbatore 641 003, Tamil Nadu, India

<sup>4</sup>Department of Seed Science and Technology, Tamil Nadu Agricultural University, Coimbatore 641 003, Tamil Nadu, India

\*Correspondence email - [vigneshagri119@gmail.com](mailto:vigneshagri119@gmail.com)

Received: 25 August 2025; Accepted: 09 November 2025; Available online: Version 1.0: 22 December 2025

**Cite this article:** Vignesh S, Arthanari PM, Kalpana R, Janaki P, Karthikeyan S, Umarani R. Pectin micro-encapsulation of pretilachlor for smart herbicide delivery through biopolymer guided slow release. *Plant Science Today* (Early Access). <https://doi.org/10.14719/pst.11446>

## Abstract

Conventional pretilachlor formulation faces quick dissipation, leaching, and reduced efficacy. The present study aimed to synthesize encapsulated pretilachlor using pectin to achieve sustained release by optimising counter-ion solution and herbicide concentration. Pretilachlor was microencapsulated with 6 % pectin via ionotropic gelation using 2 % calcium chloride (CaCl<sub>2</sub>), barium chloride (BaCl<sub>2</sub>), zinc sulphate (ZnSO<sub>4</sub>) and zinc acetate as cross-linking baths. Herbicide concentrations of 0.5, 1.0 and 2.0 mL were evaluated. Morphological and encapsulation properties were characterized through phase contrast microscope, field emission scanning electron microscope (FESEM), Fourier transformed infra-red (FTIR) spectroscopy and EDS. Encapsulation efficiency and release profiles were determined via UV-Vis spectrophotometry and analysed using mathematical kinetic models. The extrusion of 6 % pectin solution into 2 % cross-linking baths produced beads of varying shapes, with BaCl<sub>2</sub> yielding the most uniform and stable spherical microspheres. The mean diameter of the beads increased from 1.25 to 1.71 mm as pretilachlor concentration increased from 0.5 to 2.0 mL. Encapsulation efficiency and swelling percentage were highest at 0.5 mL concentration (69.4 % and 66.7 %), followed by 1.0 mL (64.04 % and 61.4 %) and 2.0 mL (59.36 % and 61.8 %), respectively. Structural analyses confirmed uniform encapsulation and stable microsphere formation and the encapsulated formulations exhibited a slow and sustained release pattern governed by first-order diffusion-controlled kinetics, in contrast to the rapid initial burst observed in the commercial formulation. Overall, encapsulating 0.5 mL of pretilachlor in 6 % pectin emerged as the most suitable treatment, offering improved encapsulation efficiency, higher swelling capacity and steady herbicide release for effective application.

**Keywords:** ionotropic gelation; microencapsulation; pectin; pretilachlor; slow release

## Introduction

Herbicides serve as a potential tool in the relentless battle between crops and weeds, blended with chemical science and strategic application to outsmart weed species and help achieve optimal crop yields. These innovations disrupt weed growth at the biological level, replacing labour-intensive methods with targeted efficiency. However, while herbicides control weeds effectively, excessive and continuous use poses numerous challenges. These include phytotoxicity in crops, soil and water pollution and health risks to humans and animals through food chain contamination (1, 2). Herbicides may persist in soil, affecting subsequent crops and non-target organisms and can potentially contaminate water sources through leaching (3). Moreover, intensive use of herbicides with the same mechanisms of action leads to the development of herbicide-resistant weeds and shifts in weed populations (4). Pre-emergence herbicides typically provide effective weed control for a duration of 15 to 20 days (5). However, subsequent flushes of germinating weeds can obstruct crop growth by competing for resources (6). To address this limitation and maintain a weed-free environment during the critical growth period of rice, controlled-release

formulations offer an effective strategy. Controlled-release formulations regulate the availability of active ingredients (herbicides) in soil through encapsulation techniques. In this approach, the active ingredients are enclosed within a secondary material, typically spherical carriers at the nanoscale/microscale, allowing their controlled release. This strategy enhances weed control, stabilizes the active ingredients, reduces environmental loss and minimizes herbicide usage and decreases soil residue and phytotoxicity (7).

In the quest for higher yields and cleaner fields in rice ecosystems, pretilachlor (C<sub>17</sub>H<sub>26</sub>ClNO<sub>2</sub>) stands out as a powerful pre-emergent herbicide (8). It belongs to the acetanilide group, widely employed to control annual grasses, sedges and broadleaf weeds in transplanted and direct-seeded rice (9). Direct-seeded rice (DSR) is becoming more prevalent due to labour and water scarcity, but the risk of yield loss from weeds in direct-seeded rice is greater than in transplanted rice (10). Yield losses due to weeds in DSR can range from 10-100 % without control measures (11). With reports of up to 96 % loss in dry DSR and 61 % in wet DSR (12). Controlling weeds in rice during the critical period assumes greater importance for

obtaining a higher yield. In direct-seeded rice, the critical period for mixed weed infestations extends from 12-60 days after seeding (13). Pretilachlor, with its ability to inhibit the synthesis of fatty acids needed for cell membranes and other lipid-containing structures in susceptible weeds, primarily grassy weeds in rice crops, by interfering with the acetyl-CoA carboxylase (ACCase) enzyme (14). It offers early-season control that reduces competition during the crops' most vulnerable stages. Its primary dissipation pathway in soil is due to microorganisms (15). Pretilachlor dissipates rapidly in paddy water, with a half-life of 4.68-6.77 days, while persisting longer in sediment with a half-life of 15.01-28.76 days (13). However, it is toxic to aquatic mammals and fish when it leaches into the water bodies. Herbicides often enter natural waters through irrigation, posing environmental risks (9). To mitigate its adverse effects and improve the efficacy, encapsulation of pretilachlor with hydrophilic polymers will be a potential approach as it reduces the leaching loss, photodegradation and prolong the half-life of herbicide to improve the efficiency of herbicide effect. Therefore, pretilachlor is encapsulated with suitable polymers to enhance sustained release, improve efficacy and minimize environmental impact, making it a key tool in modern, sustainable weed management strategies.

Various organic and inorganic polymers are used for herbicide encapsulation. Some studies have explored the encapsulation of pretilachlor using various polymers and techniques. For instance, polyurea, a synthetic polymer, was used to synthesise pretilachlor microcapsule suspension through the interfacial polymerisation technique (16). Polyethylene glycol (PEG), a synthetic polymer, was used to encapsulate pretilachlor through microemulsion and monolithic dispersion (17). The synthetic polymers like polycaprolactone (PCL) and poly allylamine hydrochloride (PAH) + poly sodium (styrene sulfonate) (PSS) were utilised to encapsulate pretilachlor (18). All these studies have used organic synthetic polymers, as most of them are petrochemical-based polymers. However, the knowledge on the encapsulation of pretilachlor in pectin is lacking. Pectin is an organic polymer widely used as a carrier in the pharmaceutical field and food industries. It is now being explored for use in agrochemicals. It comprises chains of D-galacturonic acid units, which are linked by  $\alpha$ -(1-4) glycosidic linkage (19). Pectin is derived from plant sources (e.g., citrus peels, apple pomace) and is fully biodegradable and eco-friendly, breaking down naturally without leaving toxic residues, non-toxic and safe for humans, animals and soil microbes. Pectin is an ideal polymer due to its greater stability in acidic conditions and high temperature, gelation property and biocompatibility. Since it is abundantly available as a byproduct of fruit processing, pectin is relatively low-cost compared to specialized synthetic polymers (20). Hence, this study was designed to develop pectin-based encapsulation of pretilachlor.

## Materials and Methods

### Materials

Herbicide pretilachlor 50 % EC (Taghit) was purchased from Tropical Agrosystem (India) Private Limited. Pectin was purchased from Isochem Laboratories, Angamali, Kochi. All other chemicals used were analytical grade, purchased from Sigma Aldrich. Deionised water was used for the synthesis of pectin polymeric microsphere and pectin encapsulated pretilachlor microsphere. The chemicals used in the study were pretilachlor, pectin, zinc acetate, zinc

sulphate, calcium chloride (anhydrous) and BaCl<sub>2</sub>.

### Methods

#### Encapsulation of pretilachlor in pectin microspheres

Pectin microspheres and herbicide encapsulation were prepared based on the earlier protocol with some modifications through the ionotropic gelation method (21). Pectin (6 g) was dissolved in 100 mL of deionised water by stirring at 400 rpm using a magnetic stirrer to obtain a uniform mixture. 6 % pectin was extruded dropwise at 4 mL min<sup>-1</sup> through a syringe with a needle (0.55 mm) into the 2 % counter ion solutions (BaCl<sub>2</sub>, CaCl<sub>2</sub>, ZnSO<sub>4</sub> and zinc acetate), maintaining the collection distance of 4-5 cm from the bath solutions. Different-shaped (flat and distorted, spherical, spherical with a chained tail and tear drop) pectin microspheres were formed instantly in each gelation bath solution (CaCl<sub>2</sub>, BaCl<sub>2</sub>, zinc acetate and ZnSO<sub>4</sub>, respectively). The microspheres were washed after curing for 30 min in the gelation bath with deionised water and ethanol. Then, microspheres were dried at room temperature until a constant weight was achieved through successive measurements. The microspheres were stored in an airtight container at room temperature for further characterisation. Similarly, 6 % pectin solution was prepared and herbicide (pretilachlor) was added slowly into the pectin solution at three different concentrations (0.5, 1.0, 2.0 mL). Encapsulated pretilachlor microspheres were prepared by dripping the different concentrations of pretilachlor mixed with pectin solution into 2 % barium chloride (BaCl<sub>2</sub>) solution. After curing and washing, each concentration of encapsulated pretilachlor microspheres was dried and stored for further evaluation.

#### Encapsulation efficiency of pretilachlor in pectin microspheres

Encapsulation efficiency represents the amount of pretilachlor encapsulated in pectin microspheres. Encapsulation efficiency of pretilachlor-loaded microspheres of varying concentrations was analysed individually using a UV-Vis spectrophotometer (Agilent, Cary 60 UV-Vis spectrophotometer). Two sets of standards were prepared, one with pretilachlor 50EC from 1 to 10 ppm using water and another with technical grade pretilachlor prepared from 1 to 10 ppm using acetonitrile, for assessing the wavelength of maximum absorption through spectrum scanning with a wavelength of 190 to 800 nm in UV-Vis spectroscopy. The known concentrations of pretilachlor (1, 2, 4, 8 and 10 ppm) technical grade standards were used to find OD values in UV Vis spectrophotometer and obtained a standard curve (min R<sup>2</sup> = 0.95). 10 mg of each pectin encapsulated pretilachlor was dissolved in 50 mL of distilled water after grinding using a pestle and mortar and kept under continuous magnetic stirring for 8-12 hr for complete dissolution of microspheres. Aliquot was filtered through a membrane filter (0.22  $\mu$ m) to reduce the residual interaction after centrifuging at 3000 rpm for 30 min and analysed its concentrations at  $\lambda_{max}$  = 194 nm using a UV-Vis spectrophotometer. Pretilachlor encapsulation efficiency was calculated using the following formula (Eqn. 1).

Encapsulation efficiency (%) =

$$\frac{\text{Amount of herbicide encapsulated (g)}}{\text{Amount of herbicide used for encapsulation (g)}} \times 100$$

(Eqn. 1)

### Swelling behaviour of pectin and pretilachlor encapsulated microspheres

The swelling properties of pretilachlor-loaded and empty pectin microspheres were assessed in terms of the change in weight of microspheres as a function of time. Measurements of the initial weight of dried and final weight of wet microspheres were made before and after microspheres were soaked in water at room temperature in distilled water, respectively. The microspheres were retrieved from the water at regular intervals to assess the change in weight at time 't'. The swelling percentage was calculated using the following formula (Eqn. 2).

$$\% \text{ swelling} = \frac{\text{Weight of beads at time (g)} - \text{Initial weight of beads (g)}}{\text{Weight of beads at time "t" (g)}} \times 100 \quad (\text{Eqn. 2})$$

### Characterisation of pretilachlor-loaded pectin beads

The size and shape of the pectin microsphere and pectin encapsulated pretilachlor microspheres were examined using a phase contrast microscope (LEICA DM2000 LED coupled with imaging software Capture V2.4) at 5 x magnification. The surface topography of pectin encapsulated pretilachlor beads was assessed using a field emission scanning electron microscope (FESEM) without coating. Electron microscopy images were obtained at an acceleration voltage of 15.0 kV with different magnifications (130 x, 246 x, 2.54 kx, 5.00 kx). Fourier transformed infra-red (FTIR) spectra of pectin beads and pretilachlor-loaded pectin beads were recorded using SHIMADZU-FTIR to ensure the encapsulation of pretilachlor in the pectin polymeric system. Attenuated total reflection (ATR) mode was used at a wavenumber regime of 4000 to 400 cm<sup>-1</sup>. Further, the elemental composition of encapsulated pretilachlor in pectin beads was recorded using energy dispersive X-ray analysis or energy dispersive X-ray spectroscopy (EDAX/EDS).

### Herbicide release test of encapsulated pretilachlor microspheres

#### Release pattern in aqueous medium

Release pattern of the encapsulated pretilachlor at three concentrations (0.5, 1 and 2 mL) was studied in the laboratory by comparing with commercial pretilachlor 50 EC at three concentrations (0.5, 1 and 2 mL) to assess the slow release of encapsulated pretilachlor from the pectin microsphere. 30 mg of pretilachlor-loaded beads were placed in one litre of deionised water (aqueous medium). The dissolution bath was maintained at room temperature and shaken at 100 rpm using a mechanical shaker. Similarly, an equivalent quantity of active ingredient from commercial pretilachlor was also placed in the dissolution medium to compare the release pattern of both formulations in water. Aliquots of 10 mL were withdrawn at time intervals of 2, 4, 6, 8, 10, 12, 24, 48, 72 and 96 hr, with an equal volume of deionised water added back after each withdrawal. The concentration of herbicide release from the encapsulated pretilachlor pectin matrix and commercial formulation in the water system at the mentioned time intervals was assessed through a UV-Vis spectrophotometer at 194 nm ( $\lambda_{\text{max}}$  obtained through spectrum scanning).

#### Release kinetics with mathematical models

The concentration of pretilachlor released from the sample at defined time intervals was used to determine the percentage of

pretilachlor released from the pectin matrix. Data from different concentrations of encapsulated pretilachlor (0.5, 1.0, 2.0 mL) were used to construct graphs according to the mathematical models, including zero-order (Eqn. 3), first-order (Eqn. 4), Higuchi (Eqn. 5) and Korsmeyer-Peppas (Eqn. 6) models (22-25). These analyses provide information on the release mechanism.

$$f_t = K_0 t \quad (\text{Eqn. 3})$$

$$\ln Q_t = \ln Q_0 + K_1 t \quad (\text{Eqn. 4})$$

$$f_t = K_H t^{1/2} \quad (\text{Eqn. 5})$$

$$M_t / M_\infty = K t^n \quad (\text{Eqn. 6})$$

Where, in equation (3),  $f_t$  is the fraction of drug released at time  $t$  and  $K_0$  is the zero-order release constant. In equation (4),  $Q_t$  is the amount of drug remaining to be released at time  $t$ ;  $Q_0$  is the drug amount remaining to be released at zero hr;  $K_1$  is the first-order release constant. In equation (5),  $f_t$  is the fraction of drug release at time  $t$ ;  $K_H$  is the Higuchi release rate constant. In equation (6),  $M_t$  is the amount released at time  $t$ ;  $M_\infty$  is the amount released at infinite time;  $K$  is the Korsmeyer-Peppas release constant;  $n$  is the release exponent.

## Results and Discussion

### Encapsulation of pretilachlor in pectin microsphere

Encapsulation of pretilachlor in pectin polymeric microspheres was carried out through the ionic gelation technique. The different ion gelation bath affects the shape and behaviour of pectin microspheres without loading pretilachlor. Fresh and dried pectinate microspheres without loading pretilachlor cross-linked with different counter ions gelation bath are illustrated in Fig. 1 & 2. The pectin beads formed with 2 % CaCl<sub>2</sub> crosslinking agent are irregular, translucent elongated in shape. This might be due to higher viscosity and low surface tension of pectin solution or the concentration of both pectin and CaCl<sub>2</sub> solution. Higher calcium concentrations typically create more rapid surface gelation, potentially leading to irregular shapes (26). The pectin beads formed with 2 % zinc acetate crosslinking agent are spherical in shape with a chain-like tail. Similarly, in 2 % zinc sulphate crosslinking agent tear-drop-like shaped beads were formed. Whereas the pectin beads formed with 2 % BaCl<sub>2</sub> shows proper spherical to oblate shape microsphere (Fig. 3). Therefore, the different concentration of pretilachlor (0.5, 1 and 2 mL) was encapsulated in 6 % pectin polymer with 2 % BaCl<sub>2</sub> gelation bath and the microspheres obtained were spherical to oblate in nature irrespective of pretilachlor concentrations (Fig. 4 & 5) but with varying size ( $1252.17 \pm 7.90$ ,  $1451.28 \pm 0.08$ ,  $1708.70 \pm 6.25$   $\mu\text{m}$ ) due to increasing pretilachlor concentrations, respectively (Fig. 6 and Table 1). Intermolecular crosslinking between the carboxyl groups of pectin and divalent cation barium takes place due to polyanion cation interactions. Unbranched non-esterified galacturonan units in pectin are involved in the complexing reactions with divalent ions. The shape of the microsphere formed is primarily due to this process and the interplay between the pectins' structure and the continuous aqueous phase.

### Encapsulation efficiency of pretilachlor in pectin microspheres

A comparison of encapsulation efficiency for various concentrations of pretilachlor loaded in pectin polymeric microspheres is shown in Fig. 7. The encapsulation efficiency of pretilachlor decreases with



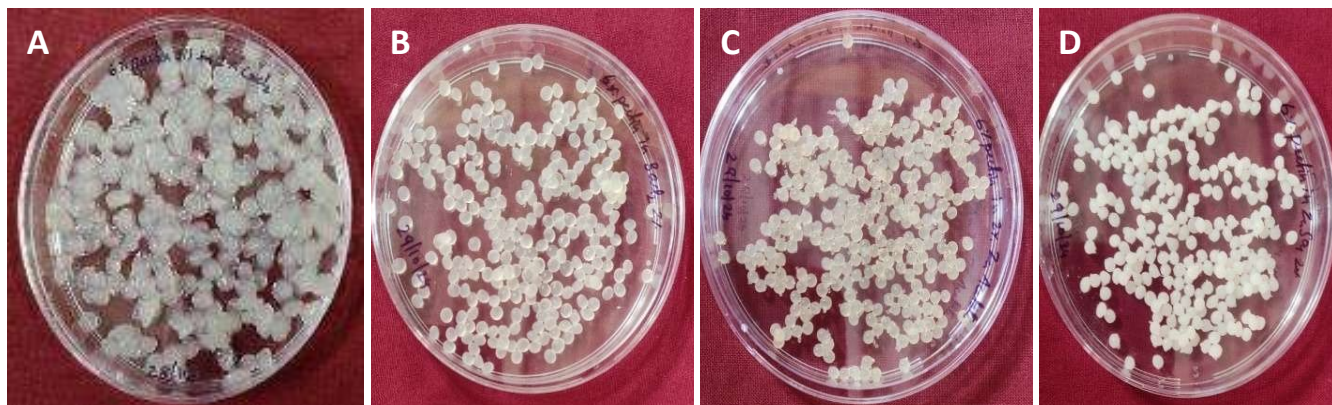


**Fig. 1.** Fresh wet pectinate beads without pretilachlor at 2 % of different gelation bath: **A.**  $\text{CaCl}_2$ , **B.**  $\text{BaCl}_2$ , **C.** zinc acetate, **D.**  $\text{ZnSO}_4$ .

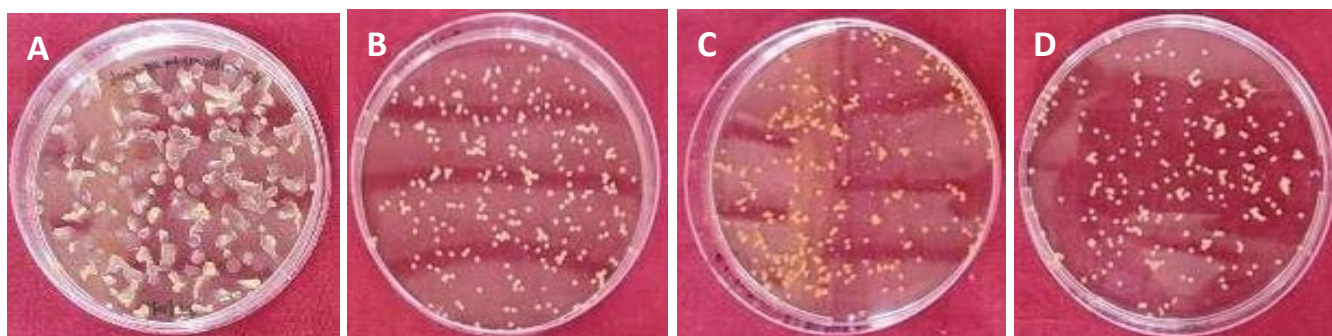


**Fig. 2.** Dry pectinate beads without pretilachlor at 2 % of different gelation bath: **A.**  $\text{CaCl}_2$ , **B.**  $\text{BaCl}_2$ , **C.** zinc acetate, **D.**  $\text{ZnSO}_4$ .

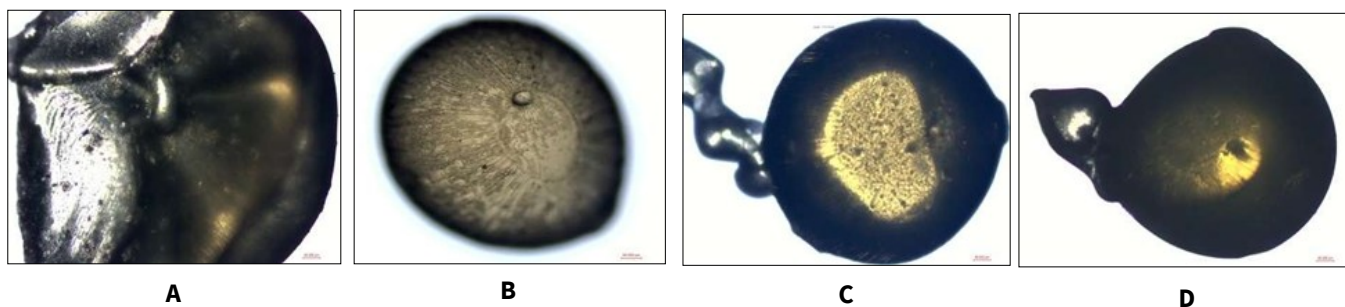


**Fig. 3.** Phase contrast microscopic image of pectin polymeric microspheres in different crosslinking agents of 2 %: **A.**  $\text{CaCl}_2$ , **B.**  $\text{BaCl}_2$ , **C.** Zinc acetate, **D.**  $\text{ZnSO}_4$ .

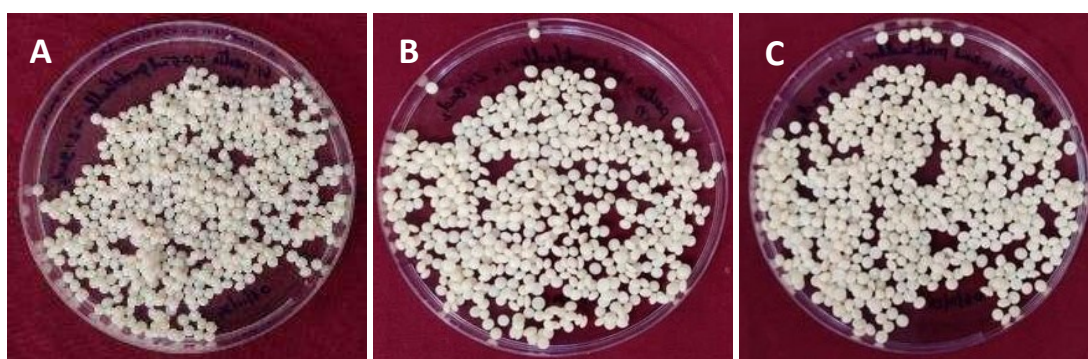


**Fig. 4.** Fresh wet pectinate beads loaded with different concentrations of pretilachlor in 2 %  $\text{BaCl}_2$ : **A.** 0.5 mL, **B.** 1 mL, **C.** 2 mL.

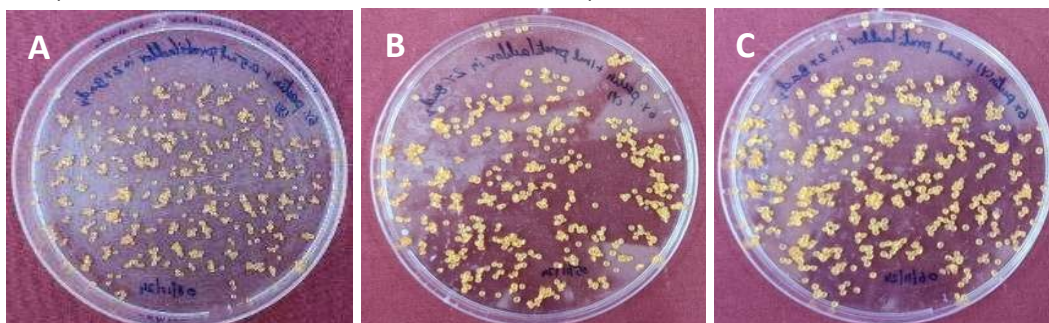


**Fig. 5.** Dry pectinate beads loaded with different concentrations of pretilachlor in 2 %  $\text{BaCl}_2$ : **A.** 0.5 mL, **B.** 1 mL, **C.** 2 mL.



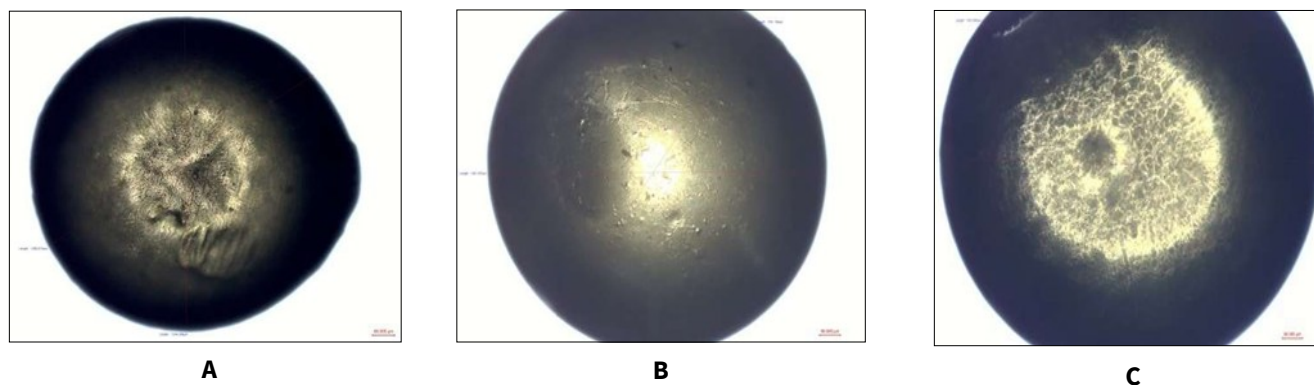


**Fig. 6.** Phase contrast microscopic image of 0.5, 1.0 and 2.0 mL pretilachlor loaded in pectin microsphere: **A.** Encapsulated pretilachlor microsphere (0.5 mL), **B.** Encapsulated pretilachlor microsphere (1.0 mL), **C.** Encapsulated pretilachlor microsphere (2.0 mL).

**Table 1.** Impact of varying pretilachlor loading concentrations on the dimensions and form of pectin-encapsulated pretilachlor microspheres

BaCl <sub>2</sub> concentration	Pretilachlor concentration	Diameter (μm)	Remarks
2 %	0.5 mL	1252.17 ± 7.90	Beads were spherical to oblate shape
	1.0 mL	1451.28 ± 0.08	
	2.0 mL	1708.70 ± 6.25	

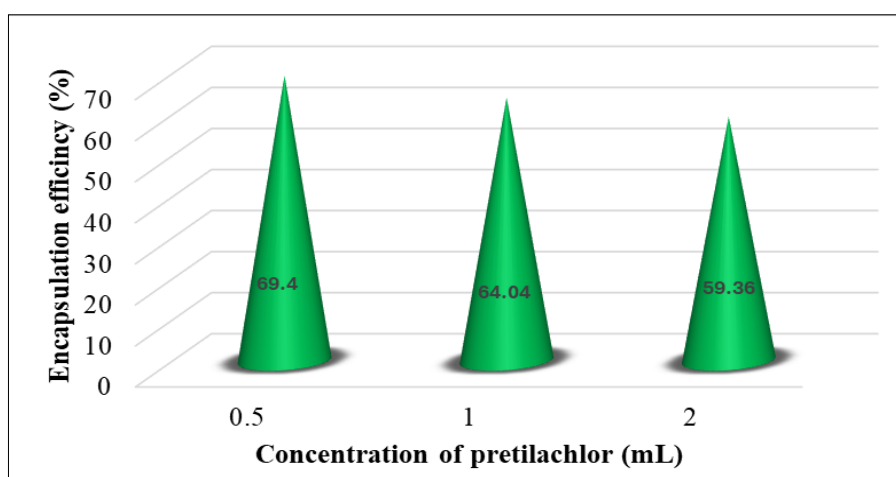


**Fig. 7.** Impact of herbicide concentration on pretilachlor encapsulation efficiency in pectinate microspheres.

increasing concentration of pretilachlor in pectin microspheres. The higher concentration of pretilachlor increases the drug-to-polymer ratio, thereby reaching saturation and decreasing the encapsulation efficiency. Higher encapsulation efficiency (69.4 %) of pretilachlor was noticed in microspheres loaded with 0.5 mL pretilachlor followed by 1.0 mL pretilachlor with an encapsulation efficiency of 64.04%. The lowest encapsulation efficiency (59.36 %) was observed in microspheres with loading of pretilachlor at 2 mL concentration, might be due to efflux of pretilachlor molecules out of polymeric system to achieve equilibrium diffusion coefficient with surrounding ion gelation bath. Encapsulation efficiency varies depending on factors such as polymer type, herbicide solubility and polymer concentration, typically ranging from 24.7 to 63 % (27, 28). Similarly, Research indicates that encapsulation efficiency decreases with increasing concentration of herbicide load (29, 30).

#### Swelling behaviour of pectin beads and encapsulated herbicide beads

Water uptake by polymeric systems determines the release pattern of encapsulated materials (31). The effect of various concentrations of pretilachlor on the swelling behaviour of pretilachlor-loaded and unloaded microspheres is shown in Fig. 8. The percentage of swelling increases with time for the first four hours, irrespective of the concentration of pretilachlor. Higher swelling percentage (65.1 to

66.7 %) was observed at 2 to 6 hr in microspheres cross-linked with 2 % BaCl<sub>2</sub> at 0.5 mL pretilachlor concentrations in comparison with pretilachlor unloaded and loaded microspheres of 1.0 and 2.0 mL concentrations. These findings correlated with the previous study, indicating that higher herbicide loading reduces water uptake by the polymer (32). This effect is attributed to the herbicides' impact on drug diffusion rather than polymer relaxation (33). The presence of herbicides can alter the three-dimensional membrane structure of superabsorbent polymers, affecting their water-absorbing capacity (34). The swelling process is characterised by an initial rapid increase followed by a gradual approach to equilibrium, with the equilibrium swollen value being affected by drug loading levels. The reduced swelling of pretilachlor-loaded microspheres at higher drug concentrations might be due to densification of the polymer network or specific drug-polymer interactions.

#### Characterisation of encapsulated pretilachlor microspheres

Field emission scanning electron microscope images of encapsulated pretilachlor in pectin polymeric microspheres are illustrated in Fig. 9. The microsphere at 130 x and 246 x magnification (Fig. 9A, 9B) exhibits a nearly perfect circular shape with a distinctive central hole/depression and radial striations extend from the centre to the periphery, suggesting controlled cross-linking between pectins' carboxyl groups and Ba<sup>2+</sup> ions that created stronger ionic

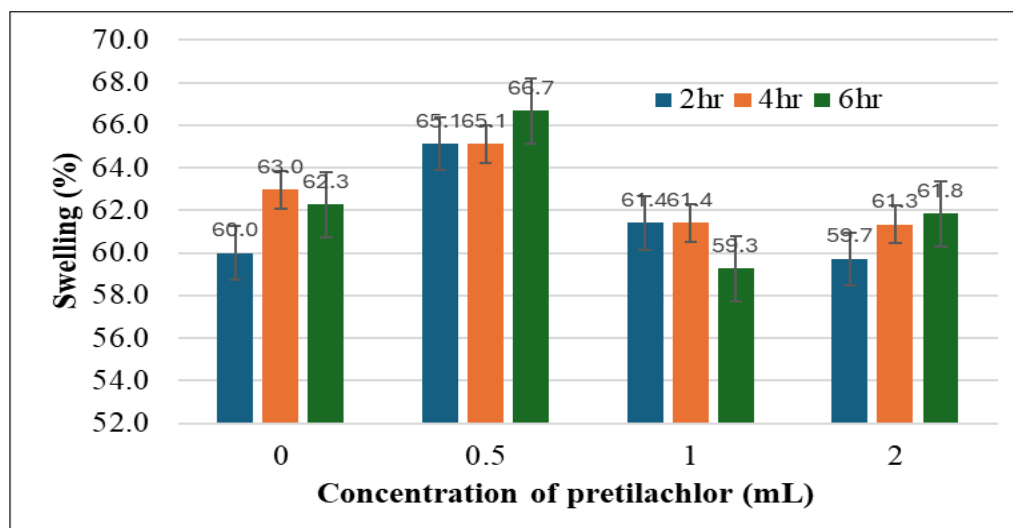
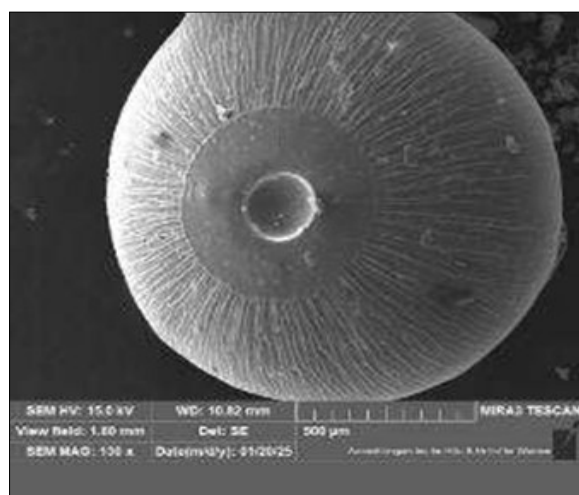


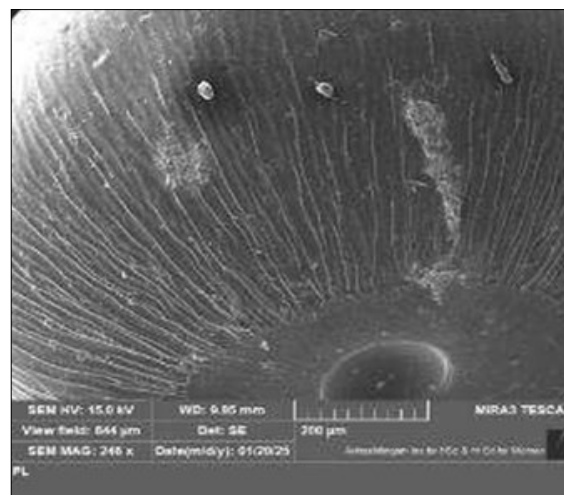
**Fig. 8.** Influence of pretilachlor concentration on pectin microsphere and pectin-encapsulated pretilachlor microsphere swelling behaviour.

bridges with pectin chains. The central depression likely formed during solvent evaporation, creating a hollow or less dense core beneficial for controlled release (35). Its intact structure indicates good stability. The microsphere shows minimal surface porosity but pronounced texture. The radial striation may create microchannels that could influence pretilachlor release kinetics (36). Surface roughness appears relatively uniform, suggesting a homogeneous distribution of the encapsulated herbicide. The structured morphology suggests potential for controlled release of pretilachlor, which could extend herbicidal activity.  $Ba^{2+}$  cross-linking may provide greater stability in soil environments (37). The uniform shape

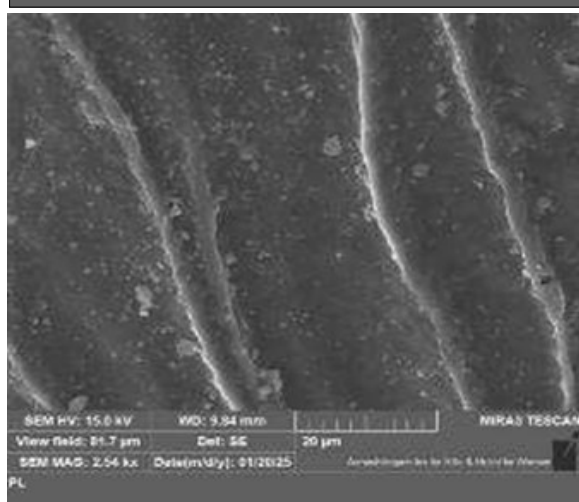
indicates well-controlled droplet formation during the gelation process. Fig. 9C shows distinct parallel ridge formations on the surface, which may represent areas of higher cross-linking density between pectin chains and  $Ba^{2+}$  ions. Small particulate matter (bright spots) on the surface suggests potential surface-adsorbed pretilachlor or partial crystallisation (Fig. 9D). The channel-like structures could facilitate controlled release through surface erosion (38). The varied morphology could provide both immediate release (surface drug) and sustained release (matrix-embedded drug). In addition to surface morphology study, further analysis, like EDS and FTIR, was carried out.



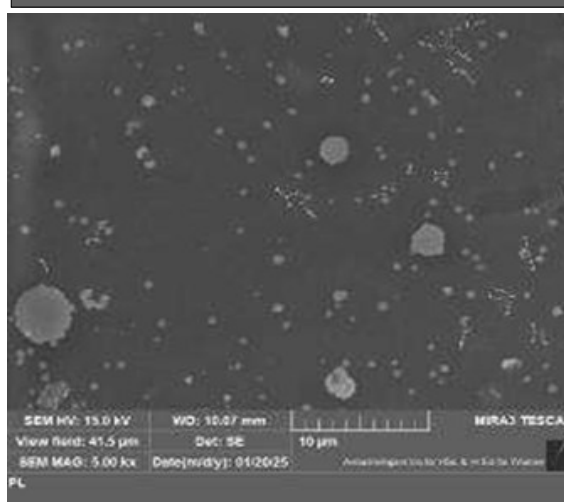
A



B



C



D

**Fig. 9.** FE-SEM micrographs of encapsulated pretilachlor in pectin polymer microsphere at different magnification, **A.** 100 x, **B.** 246 x, **C.** 2.54 kx, **D.** 5.00 kx magnification.

Elemental composition analysis was performed to ensure the encapsulated pretilachlor in pectin polymer microspheres. Energy dispersive X-ray spectroscopy image of pectin microspheres cross-linked with barium (Ba) without pretilachlor encapsulation and the pretilachlor encapsulated pectin microspheres are illustrated in Fig. 10A and 10B. Pectin microspheres without pretilachlor (Fig. 10A) are composed of 47 % oxygen (O), 15 % carbon (C), 17 % chlorine (Cl), 15 % Ba and 5 % molybdenum (Mo). The Ba:Cl ratio is approximately 1:1.13, close to the expected 1:2 ratio in  $\text{BaCl}_2$ , suggesting some chloride was washed away during preparation. The high oxygen percentage indicates abundant available carboxyl groups in pectin for ionic interaction with  $\text{Ba}^{2+}$ . The even distribution of Ba (likely shown in light blue based on the legend) confirms homogeneous cross-linking throughout the structure. The coloured mapping suggests no significant segregation or clustering of components, indicating efficient gelation. Strong peaks for C and O confirm the organic pectin matrix, the well-defined Ba peaks at approximately 4.5 keV (L-shell) and additional peaks at higher energy levels confirm Ba incorporation (39). The presence of Cl peaks validates residual chloride from the cross-linking solution. The relatively high Ba content suggests extensive cross-linking, which would contribute to structural stability (40). The balanced elemental composition suggests a complete reaction between pectin and  $\text{BaCl}_2$ . The EDS analysis provides valuable compositional data complementary to the morphological information from SEM. The combined analysis confirms successful formation of Ba-crosslinked pectin microspheres through ionotropic gelation.

Encapsulated pretilachlor in pectin microspheres (Fig. 10B) are composed of 50 % oxygen (O) highest proportion, derived from pectins' hydroxyl and carboxyl groups, 25 % C from both pectins' polysaccharide backbone and pretilachlors' organic structure, 14 % Cl from both  $\text{BaCl}_2$  crosslinker and pretilachlors' chlorinated structure, 9 % Ba cross-linking counter-ion, 2 % nitrogen (N) likely from pretilachlors' chemical structure. The detection of nitrogen (2 %) provides direct evidence of pretilachlor incorporation, as pectin lacks nitrogen while pretilachlor contains nitrogen in its molecular structure. The C:O ratio (25:50 or 1:2) is higher than would be expected (15:47 or 1:3.1) for pure pectin, suggesting the additional C content from pretilachlor (41). The presence of Cl is also partially attributable to pretilachlors' chlorinated structure in addition to residual chloride from  $\text{BaCl}_2$ . The EDS mapping shows a relatively homogeneous distribution of elements throughout the microsphere. The even distribution of colours in the surrounding matrix indicates that pretilachlor is well-dispersed within the pectin network. The maintained structural integrity despite herbicide incorporation suggests compatible interactions between pectin, Ba ions and pretilachlor.

The reduced Ba content (9 % vs 15 % in non-loaded microspheres) suggests pretilachlor may compete with pectin for interaction with  $\text{Ba}^{2+}$  ions. The oxygen-rich composition (50 %) indicates abundant hydroxyl and carboxyl groups, which could potentially support higher herbicide loading in optimised formulations. The detectable nitrogen level (2 %) suggests moderate but significant herbicide loading efficiency (42). EDS thus confirms successful encapsulation with stable incorporation.

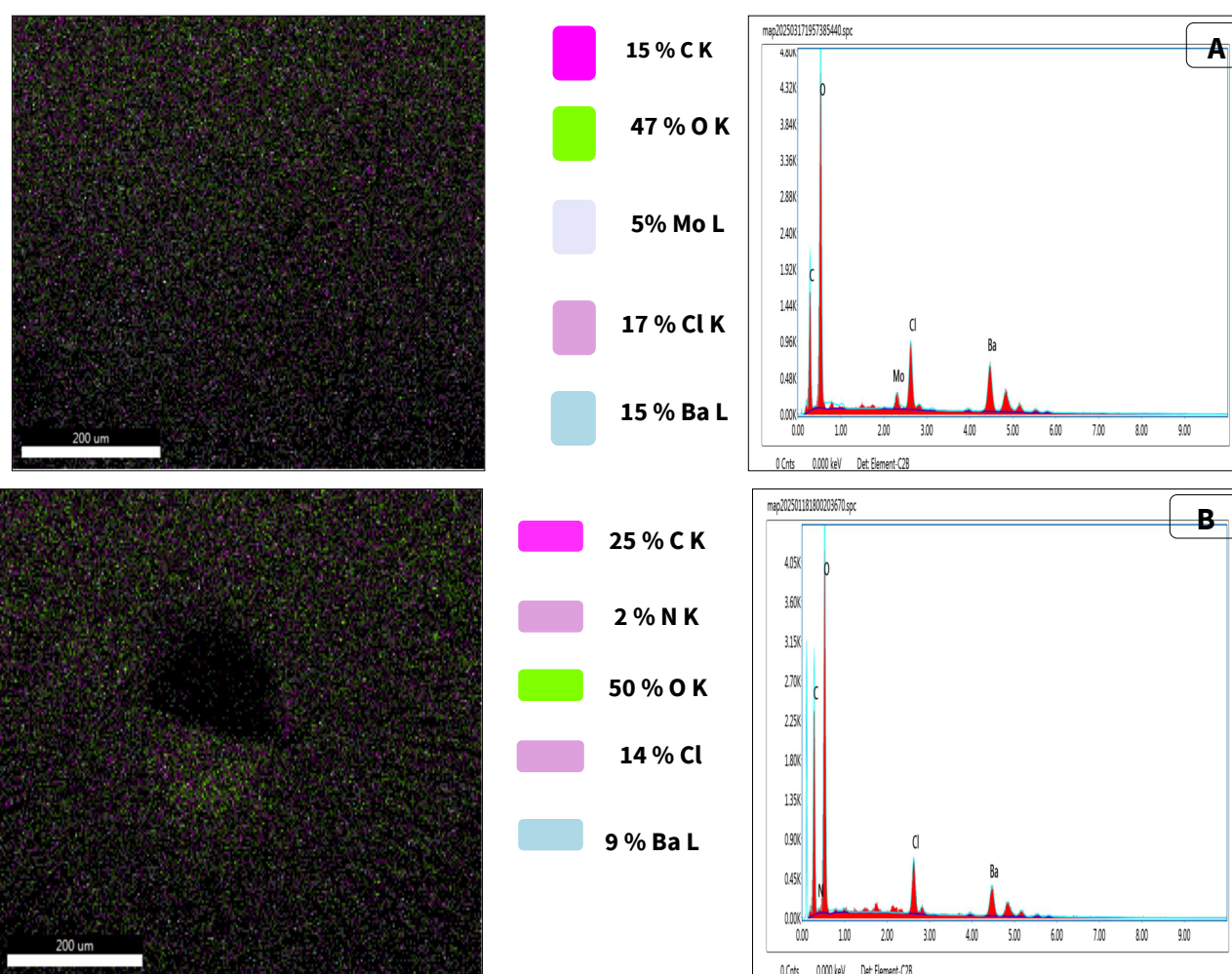


**Fig. 10.** EDX spectrum and elemental overlay: **A.** Pectin microsphere without pretilachlor, **B** Pectin encapsulated pretilachlor microsphere.



The FTIR analysis provides strong evidence for the formation of pectin-barium microspheres through ionic gelation, with the Ba ions serving as cross-linking agents between the carboxylate groups of adjacent pectin chains (Fig. 11A). The broad absorption band around 3400-3500  $\text{cm}^{-1}$  (visible at approximately 3402  $\text{cm}^{-1}$ , 3389  $\text{cm}^{-1}$ ) corresponds to O-H stretching vibrations of hydroxyl groups in the pectin structure (43). The peaks around 2930  $\text{cm}^{-1}$  (2938  $\text{cm}^{-1}$ ) can be attributed to C-H stretching vibrations of the  $\text{CH}_2$  groups in the pectin backbone. A band around 1730-1740  $\text{cm}^{-1}$  likely represents C=O stretching of the ester carbonyl groups (methyl ester) in pectin (44, 45). The absorption at approximately 1630  $\text{cm}^{-1}$  (visible around 1600-1650  $\text{cm}^{-1}$  region) corresponds to the asymmetric stretching vibration of carboxylate groups ( $\text{COO}^-$ ) (46). Bands around 1420-1450  $\text{cm}^{-1}$  can be attributed to the symmetric stretching of carboxylate groups (47). The fingerprint region (1200-950  $\text{cm}^{-1}$ ) shows characteristic peaks related to C-O stretching and C-C stretching in the polysaccharide structure of pectin. The sharp peaks at 1085  $\text{cm}^{-1}$  and 1050  $\text{cm}^{-1}$  (approximated from the spectrum) are typical of C-O-C stretching in the glycosidic linkages (48). The presence of carboxylate peaks indicates that the carboxylic acid groups of pectin have been ionised, which is essential for the ionic gelation process with  $\text{Ba}^{2+}$  ions. Such shifts in the carboxylate stretching bands confirm the ionic interaction between pectins' carboxyl groups and Ba ions. The maintenance of most characteristic pectin peaks suggests that the fundamental chemical structure of pectin remains intact during the gelation process. Overall, the spectrum confirms the successful Ba cross-linking while preserving pectins' structure.

The FTIR spectrum of encapsulated pretilachlor in pectin microspheres shows several characteristic absorption bands that provide evidence of both pectin and pretilachlor components in the microspheres (Fig. 11B). The broad absorption band at 3788  $\text{cm}^{-1}$  and 3649  $\text{cm}^{-1}$  can be attributed to O-H stretching vibrations from the hydroxyl groups present in the pectin structure. The peak at 3448  $\text{cm}^{-1}$  is assigned to N-H stretching vibrations, which could be

associated with the secondary amine group in the pretilachlor structure (49). The absorption at 3140  $\text{cm}^{-1}$  may represent aromatic C-H stretching, consistent with the aromatic rings present in pretilachlor (50). The absence of prominent peaks in the carbonyl region (1700-1750  $\text{cm}^{-1}$ ) that would be characteristic of free pectin suggests potential interaction between the carboxyl groups of pectin and Ba ions during gelation. The peaks in the fingerprint region (1000-500  $\text{cm}^{-1}$ ) show several characteristic bands. 956  $\text{cm}^{-1}$  and 902  $\text{cm}^{-1}$  correspond to C-O-C stretching in glycosidic linkages of pectin. The peaks 763  $\text{cm}^{-1}$ , 688  $\text{cm}^{-1}$  and 648  $\text{cm}^{-1}$  could be attributed to C-Cl stretching vibrations from the chlorinated aromatic ring in pretilachlor, 601  $\text{cm}^{-1}$ , 562  $\text{cm}^{-1}$  and 509  $\text{cm}^{-1}$  may represent metal-oxygen (Ba-O) vibrations, indicating the crosslinking between Ba ions and pectin. The peak at 439  $\text{cm}^{-1}$  at the far end of the spectrum could be related to Ba-O lattice vibrations (51). The presence of both pectin-related peaks and pretilachlor-specific absorptions confirms the successful encapsulation of the herbicide within the pectin matrix. The relatively low intensity of some characteristic pretilachlor peaks suggests its entrapment within the pectin network rather than just surface adsorption. The preservation of key pretilachlor functional group signatures confirms that the encapsulation process did not cause chemical degradation of the active ingredient. The spectrum suggests effective crosslinking between pectin chains via Ba ions, which would be crucial for controlling the release kinetics of the encapsulated pretilachlor. The overall spectral pattern indicates formation of a composite material where pretilachlor molecules are physically entrapped within the three-dimensional network of Ba-crosslinked pectin.

### Herbicide release test of encapsulated pretilachlor microspheres

#### Herbicide release pattern in aqueous medium

Release pattern study of encapsulated pretilachlor, compared with commercial formulation, revealed a slow and sustained release from pectin microspheres (Fig. 12). Commercial formulation shows a

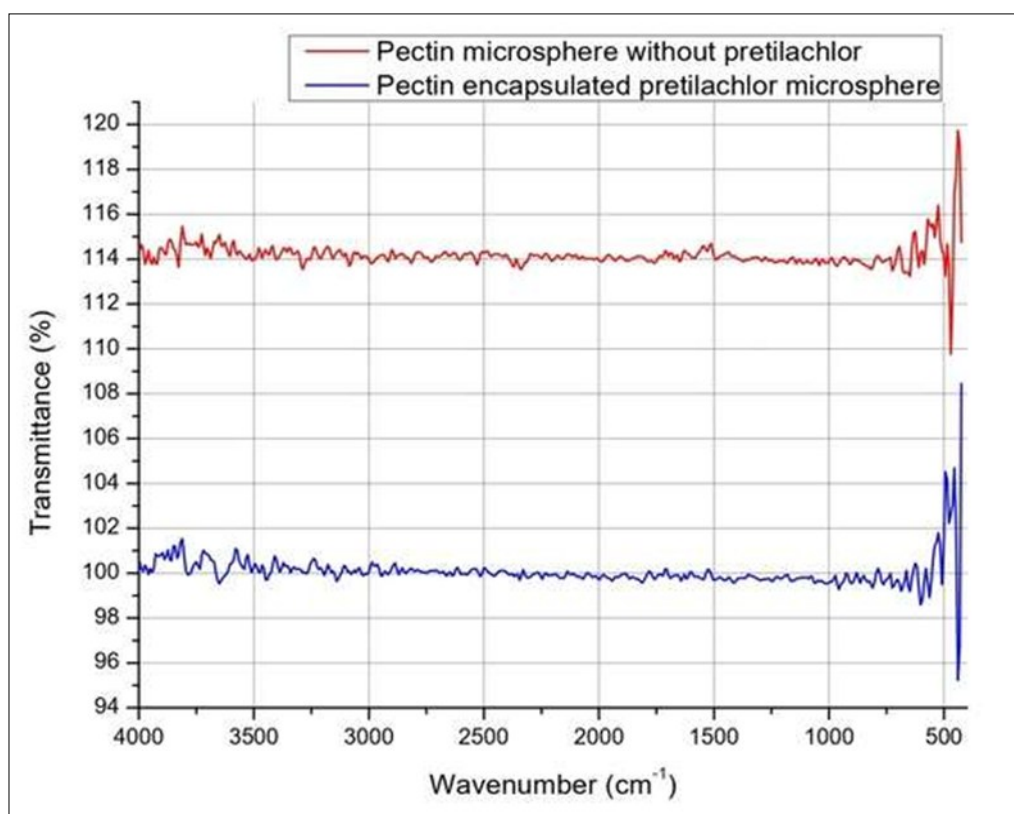


**Fig. 11.** FTIR spectrum: **A.** Pectin polymer microsphere without pretilachlor, **B.** Encapsulated pretilachlor in pectin polymer microsphere.



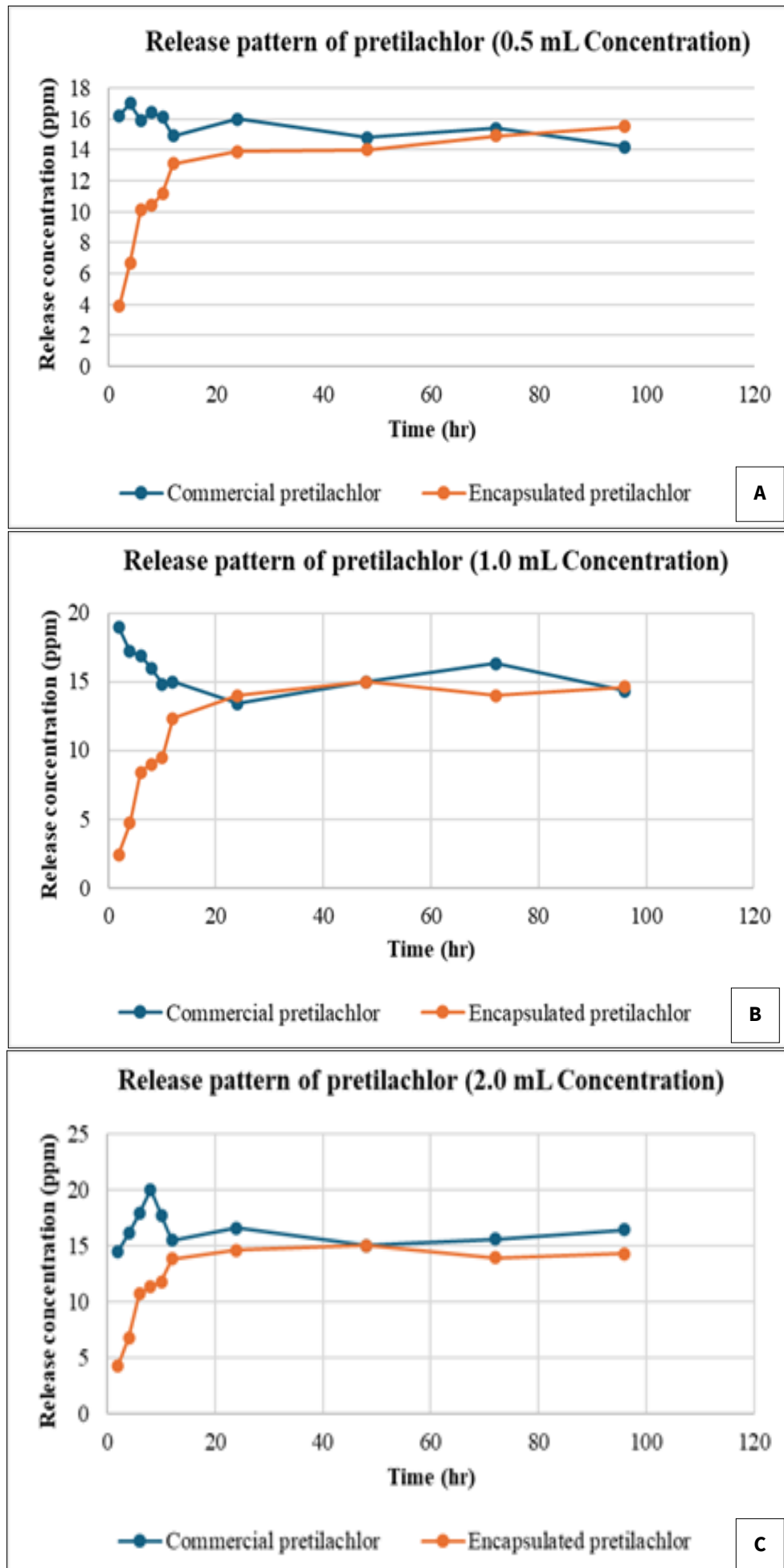


**Fig. 12.** Herbicide release pattern of commercial and encapsulated pretilachlor at different loading concentrations: **A.** 0.5 mL, **B.** 1.0 mL, **C.** 2.0 mL.

sharp initial burst, releases pretilachlor almost immediately, reaching about 15-16, ~17-18 mg/L, by 2 hr, in 0.5, 1.0 mL concentration ~20 mg/L within the first 2-8 hr in 2.0 mL concentration. Then plateaus remain essentially constant ( $15.5 \pm 0.5$  mg/L) out to 96 h in 0.5mL concentration. In 1.0 mL concentration, release declines from ~17 to ~14 mg/L for the 24 hr and maintains a steady concentration (~14-16 mg/L) through the 96 hr period with slight fluctuations. In 2.0 mL concentration, after 8 hr, there is a steady decline to ~15 mg/L for the 12 hr and maintains a steady concentration (~15-16 mg/L) through 96 hr. Encapsulated formulation shows a pronounced sustained-release profile, very low release at 0-2 hr (~4 mg/L), rapid but controlled rise between 2-12 hr, closely matching the commercial level only after 12 hr. Maintains the slow release through 96 hr and levelling off at ~15 mg/L in 0.5mL concentration. In a 1.0 mL concentration, release starts low (~2 mg/L at 2 hr) and gradually rises slowly up to 12 hr. Approaches the commercial release level by ~12-24 hr. Stabilises at around 15-16 mg/L and remains consistent up to 96 hr. In 2.0 mL concentration starts much lower (~4 mg/L at 2 hr) and steadily rises slowly up to 12 hr. Approaches ~15-16 mg/L by ~12-24 hr, then remains stable up to 96 hr. Mirrors the commercial formulations' long-term release level, but without the initial spike.

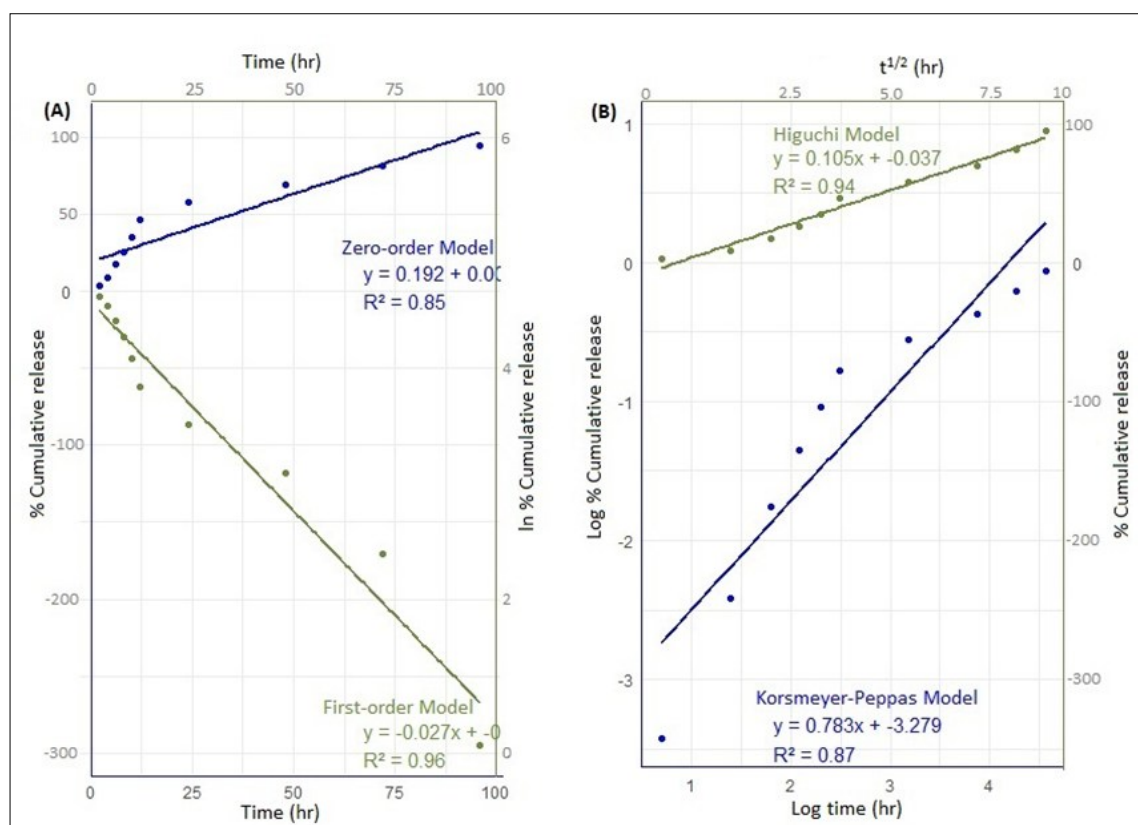
This release pattern study suggests that the commercial formulations display a sharp burst release in the first few hours, especially at higher doses (1.0 mL and 2.0 mL reach ~17-20 ppm within 2-8 hr), which can lead to phytotoxicity and environmental runoff. In contrast, the encapsulated formulations provide a consistent, diffusion-based release profile, slowly reaching effective concentrations (~15-16 mg/L) and maintaining them over extended periods. Despite the increase in dose from 0.5 mL to 2.0 mL, the encapsulated systems demonstrate controlled and consistent plateauing behaviour. This suggests that the pectin-based encapsulation matrix effectively regulates herbicide diffusion, producing a clear controlled-release profile and minimising sharp changes in release rate regardless of the loading concentration. The

results demonstrate that encapsulation technology effectively modifies the release pattern of pretilachlor, providing a more gradual and sustained release compared to the conventional EC formulation, which could improve both efficacy and environmental safety. Similarly, atrazine release from poly (lactic-co-glycolic acid) (PLGA) nanoparticles was reported to be slower: 50 % of pure atrazine was released after 3.5 h, whereas the encapsulated atrazine required 9 hr for the same release (52). Research indicates that the release of active ingredient metribuzin from bentonite polymer-composites (BPCs) was significantly lower compared to the commercial formulation of metribuzin (53).

#### Release kinetics with mathematical models

The mechanism of herbicide release from the different concentrations (0.5, 1.0 and 2.0 mL) of encapsulated pretilachlor in pectin polymeric microspheres was assessed through fitting the herbicide release percentage in release kinetics mathematic models (Fig. 13), shows that a determination coefficient ( $R^2$ ) of 0.96 for the first-order model, provided the best fit among the evaluated models for 0.5 mL concentration encapsulated pretilachlor. This indicates that the release rate is concentration-dependent, likely governed by diffusion and/or dissolution processes that slow over time. Higuchi model also shows a good fit ( $R^2 = 0.94$ ), indicating a diffusion-controlled release, typical for matrix-based systems (Fig. 13I.). For 1.0 mL concentration of encapsulated pretilachlor, the Higuchi model shows a best fit ( $R^2 = 0.96$ ) among other evaluated models, suggesting Fickian diffusion is the dominant release mechanism for this formulation and followed by the first-order model with  $R^2 = 0.95$ , showing that as the herbicide depletes, the release rate slows proportionally (Fig. 13II).

For a 2.0 mL concentration of encapsulated pretilachlor, among the evaluated models, the Higuchi model provided with best fit with an  $R^2 = 0.94$  (Fig. 13III). This indicates that the release follows diffusion-controlled kinetics. All three volumes (0.5, 1.0 and 2.0 mL pretilachlor encapsulation) follow the Higuchi diffusion-based



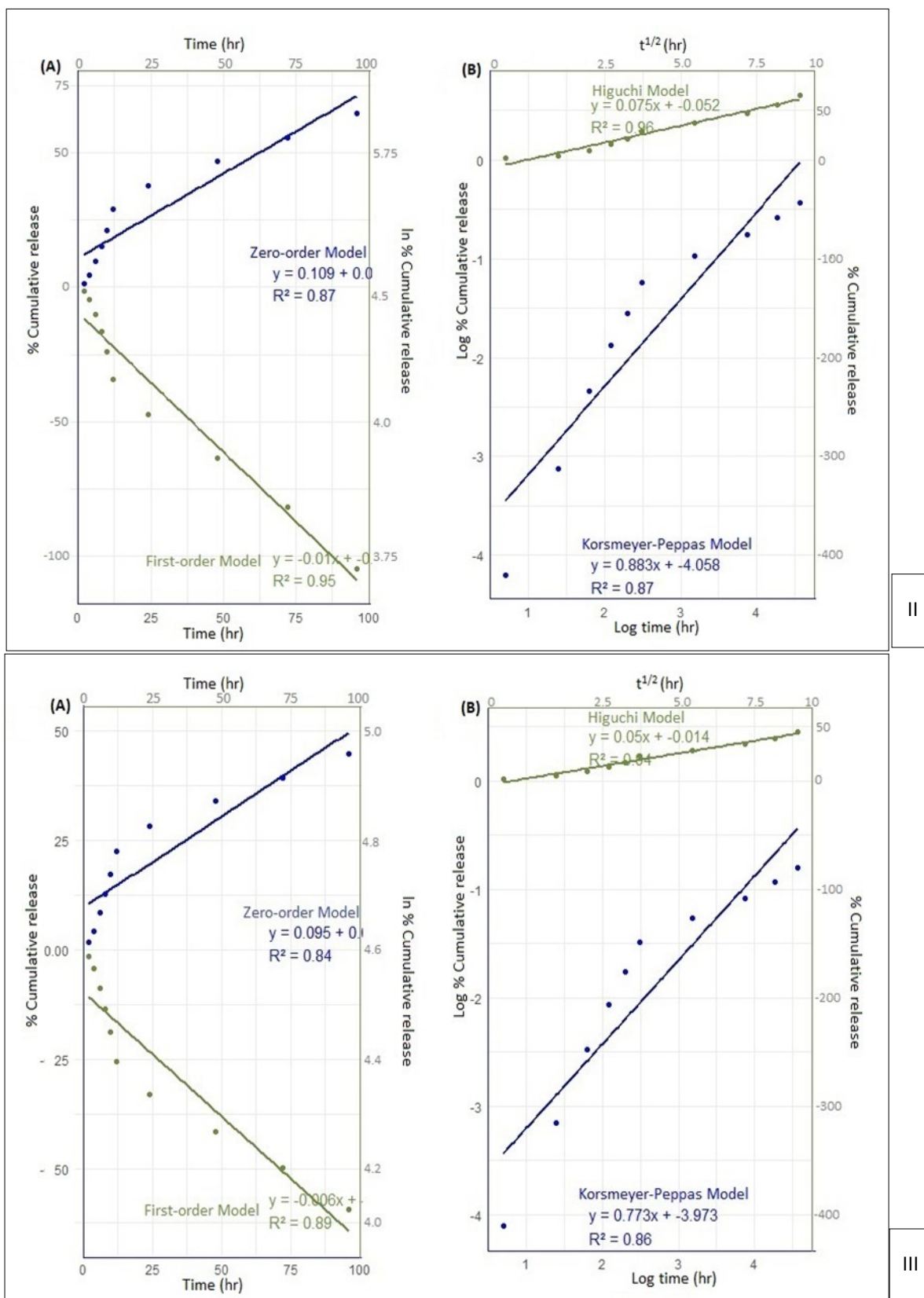


**Fig. 13.** Mathematical models of **A.** Zero-order and first-order, **B.** Higuchi and Korsmeyer-Peppas for different concentration of encapsulated pretilachlor in pectin polymer microsphere). **I.** 0.5 mL encapsulated pretilachlor, **II.** 1.0 mL encapsulated pretilachlor, **III.** 2.0 mL encapsulated pretilachlor.

model well. It describes the release based on Ficks' law of diffusion. Therefore, herbicide release from the polymeric matrix is assumed to be a diffusion-controlled process driven by the dissolution of the herbicide within the matrix and subsequent diffusion through the system. Similar findings were reported in the herbicide release mechanism of 2,4-D microparticles prepared with HPMC and CAB (54). Poly( $\epsilon$ -caprolactone) atrazine nanocapsules released the

herbicide by a combined mechanism, like diffusion and relaxation of the polymeric chains (55). Norflurazon encapsulated in ethylcellulose controlled release mechanism by diffusion (56). Diffusion-controlled metazachlor release was observed from larger particles of encapsulated metazachlor in poly (lactic acid) and gelatin (57).



## Conclusion

The pectin polymer has the potential to serve as a controlled-release system for pretilachlor herbicide. This pectin encapsulated pretilachlor will offer several potential benefits, like minimising environmental impact, improving weed control efficacy with potentially reduced herbicide dose. Among the different concentrations of encapsulated pretilachlor, the 0.5 mL loading in 6 % pectin was most effective, showing higher encapsulation efficiency, swelling percentage, steady slow herbicide release and practical advantages for field use. Also, being a small microsphere, a larger number can be obtained from unit weight, which will cover a wider area in field applications. These findings emphasise the need for further investigation to know the performance of the pectin encapsulated pretilachlor system under various environmental conditions of rice cultivation.

## Acknowledgements

All the authors are highly grateful to the Tamil Nadu Agricultural University and the Department of Agronomy, Institute Laboratory for rendering better infrastructural facilities whenever and wherever needed to do this research.

## Authors' contributions

SV carried out the synthesis and characterisation of herbicide encapsulation and also prepared the manuscript. PMA, RK & PJ participated in the sequence alignment and drafted the manuscript. SK & RU participated in the sequence alignment. All authors read and approved the final manuscript.

## Compliance with ethical standards

**Conflict of Interest:** Authors do not have any conflict of interests to declare.

**Ethical issues:** None

## References

- Hasanuzzaman M, Mohsin SM, Bhuyan MB, Bhuiyan TF, Anee TI, Masud AAC, et al. Phytotoxicity, environmental and health hazards of herbicides: challenges and ways forward. In: Prasad MNV, editor. *Agrochemicals detection, treatment and remediation*. Elsevier; 2020. p. 55–99. <https://doi.org/10.1016/B978-0-08-103017-2.00003-9>
- Brar AS. Environmental and health impacts of herbicide overuse: a review. *Journal of Agric Sustain*. 2020;15(3):112–30.
- Maheswari ST, Ramesh K. Herbicide persistence in soil and water: ecological consequences. *Environ Pollut Res*. 2018;25(4):321–35.
- Ofori R, Agyemang ED, Márton A, Pásztor G, Taller J, Kazinczi G. Herbicide resistance: managing weeds in a changing world. *Agronomy*. 2023;13(6):1595. <https://doi.org/10.3390/agronomy13061595>
- Mitra B, Patra K, Bhattacharya PM, Ghosh A, Chowdhury AK, Dhar T, et al. Efficacy of pre- and post-emergence herbicide combinations on weed control in no-till mechanically transplanted rice. *Cogent Food Agric*. 2022;8(1):2139794. <https://doi.org/10.1080/23311932.2022.2139794>
- Sairamesh K, Rao A, Subbaiah G, Rani PP. Bio-efficacy of sequential application of herbicides on weed control, growth and yield of wet-seeded rice. *J Weed Sci*. 2015;47:201–12.
- Campos EV, Ratko J, Bidyarani N, Takeshita V, Fraceto LF. Nature-based herbicides and micro-/nanotechnology fostering sustainable agriculture. *ACS Sustain Chem Eng*. 2023;11(27):9900–17. <https://doi.org/10.1021/acssuschemeng.3c02282>
- Seng CT. Inhibition of pre-emergent herbicide on weedy rice under flooded and saturated soil conditions in rice. *Sains Malays*. 2024;53(7):1525–32. <https://doi.org/10.17576/jsm-2024-5307-04>
- RajaRajeswari R, Sathiyarayanan S, Ramesh A, Ayyappan S. Evaluation of bioavailability of residues of pretilachlor in soil and water under paddy cropping condition and their influence on *Lemna gibba*. *J Agric Environ*. 2013;14:102–10. <https://doi.org/10.3126/aej.v14i0.19790>
- Chaudhary A, Venkatramanan V, Kumar Mishra A, Sharma S. Agronomic and environmental determinants of direct seeded rice in South Asia. *Circ Econ Sustain*. 2023;3(1):253–90. <https://doi.org/10.1007/s43615-022-00173-x>
- Chen G, Liu Q, Zhang Y, Li J, Dong L. Comparison of weed seedbanks in different rice planting systems. *Agron J*. 2017;109(2):620–8. <https://doi.org/10.2134/agronj2016.06.0348>
- Rathika S, Ramesh T, Shanmugapriya P. Weed management in direct seeded rice: a review. *Int J Chem Stud*. 2020;8(4):925–33. <https://doi.org/10.22271/chemi.2020.v8.i4f.9723>
- Kaur P, Kaur P, Bhullar M. Persistence behaviour of pretilachlor in puddled paddy fields under subtropical humid climate. *Environ Monit Assess*. 2015;187(8):524. <https://doi.org/10.1007/s10661-015-4756-3>
- Busi R. Resistance to herbicides inhibiting the biosynthesis of very-long-chain fatty acids. *Pest Manag Sci*. 2014;70(9):1378–84. <https://doi.org/10.1002/ps.3746>
- Hashim M, Singh V, Singh K, Dhar S, Pandey U. Weed management strategies in direct seeded rice: a review. *Agric Rev*. 2024;45(2):258–65. <https://doi.org/10.18805/ag.R-2245>
- Chen H, Liu X, Deng S, Wang H, Ou X, Huang L, et al. Pretilachlor releasable polyurea microcapsules suspension optimization and its paddy field weeding investigation. *Front Chem*. 2020;8:826. <https://doi.org/10.3389/fchem.2020.00826>
- Kumar N, Kumar R, Shakil N, Das T. Nanoformulations of pretilachlor herbicide: preparation, characterization and activity. *J Sci Ind Res*. 2016;75:676–80.
- Sowmiya S, Hemalatha M, Joseph M. Assessment of encapsulated herbicide for sustained release, weed control and crop productivity as a tool for agroecosystem biosafety. *Plant Sci Today*. 2024;11:5681. <https://doi.org/10.14719/pst.5681>
- Juneja R, Kaur M. Overview on pectin and its pharmaceutical uses. *Int J Innov Res Eng Manag*. 2022;1:353–6. <https://doi.org/10.55524/ijirem.2022.9.1.72>
- Yadav P, Pandey P, Parashar S. Pectin as natural polymer: an overview. *Res J Pharm Technol*. 2017;10(4):1225–9. <https://doi.org/10.5958/0974-360X.2017.00219.0>
- Pavithran P, Marimuthu S, R Chinnamuthu C, Lakshmanan A, Bharathi C, Kadiravan S. Synthesis and characterization of pectin beads for the smart delivery of agrochemicals. *Int J Plant Soil Sci*. 2021;33(22):136–55. <https://doi.org/10.9734/ijpss/2021/v33i2230691>
- Higuchi T. Mechanism of sustained-action medication. Theoretical analysis of rate of release of solid drugs dispersed in solid matrices. *J Pharm Sci*. 1963;52(12):1145–9. <https://doi.org/10.1002/jps.2600521210>
- Korsmeyer RW, Gurny R, Doelker E, Buri P, Peppas NA. Mechanisms of solute release from porous hydrophilic polymers. *Int J Pharm*. 1983;15(1):25–35. [https://doi.org/10.1016/0378-5173\(83\)90064-9](https://doi.org/10.1016/0378-5173(83)90064-9)
- Dash S. Kinetic modeling on drug release from controlled drug delivery systems. *Acta Pol Pharm*. 2010;67(3):217–23.
- Paarakh MP, Jose PA, Setty CM, Peterchristoper G. Release kinetics -

- concepts and applications. *Int J Pharm Res Technol*. 2018;8(1):12–20.
26. Lee BB, Chan ES. Calcium pectinate beads formation: shape and size analysis. *J Eng Technol Sci*. 2014;46(1):78–92. <https://doi.org/10.5614/j.eng.technol.sci.2014.46.1.5>
  27. Kumar S, Bhanjana G, Sharma A, Dilbaghi N, Sidhu M, Kim KH. Development of nanoformulation approaches for the control of weeds. *Sci Total Environ*. 2017;586:1272–8. <https://doi.org/10.1016/j.scitotenv.2017.02.138>
  28. Vijayamma R, Maria HJ, Thomas S, Shishatskaya EI, Kiselev EG, Nemtsev IV, et al. A study of the properties and efficacy of microparticles based on P(3HB) and P(3HB/3HV) loaded with herbicides. *J Appl Polym Sci*. 2022;139(10):51756. <https://doi.org/10.1002/app.51756>
  29. Mummasani A, Marimuthu S, Balachandar D, Radhamani S, Bharathi C, Gowtham G, et al. Microencapsulation and characterization of diclosulam in xanthan gum-based polymeric system for smart delivery of herbicide in crop production. *Int J Environ Clim Change*. 2022;12(11):1811–24. <https://doi.org/10.9734/ijec/2022/v12i1131167>
  30. Maiti S, Dey P, Banik A, Sa B, Ray S, Kaity S. Tailoring of locust bean gum and development of hydrogel beads for controlled oral delivery of glipizide. *Drug Deliv*. 2010;17(5):288–300. <https://doi.org/10.3109/10717541003706265>
  31. Grayson ACR, Cima MJ, Langer R. Molecular release from a polymeric microreservoir device: influence of chemistry, polymer swelling and loading on device performance. *J Biomed Mater Res A*. 2004;69(3):502–12. <https://doi.org/10.1002/jbm.a.30019>
  32. Issa R, Akelah A, Rehab A, Solaro R, Chiellini E. Controlled release of herbicides bound to poly[oligo(oxyethylene) methacrylate] hydrogels. *J Control Release*. 1990;13(1):1–10. [https://doi.org/10.1016/0168-3659\(90\)90069-6](https://doi.org/10.1016/0168-3659(90)90069-6)
  33. Forni F, Vandelli MA, Cameroni R. Influence of drug loading level on drug release and dynamic swelling of crosslinked gelatin microspheres. *J Microencapsul*. 1992;9(1):29–39. <https://doi.org/10.3109/02652049209021220>
  34. Liao R, Ren S, Yang P. Quantitative fractal evaluation of herbicide effects on the water-absorbing capacity of superabsorbent polymers. *J Nanomater*. 2014;2014:905630.
  35. Yun P, Devahastin S, Chiewchan N. Microstructures of encapsulates and their relations with encapsulation efficiency and controlled release of bioactive constituents: a review. *Compr Rev Food Sci Food Saf*. 2021;20(2):1768–99. <https://doi.org/10.1111/1541-4337.12701>
  36. Kumar S, Nehra M, Dilbaghi N, Marrazza G, Hassan AA, Kim K. Nano-based smart pesticide formulations: emerging opportunities for agriculture. *J Control Release*. 2019;294:131–53. <https://doi.org/10.1016/j.jconrel.2018.12.012>
  37. Deepika R, Girigoswami K, Murugesan R, Girigoswami A. Influence of divalent cation on morphology and drug delivery efficiency of mixed polymer nanoparticles. *Curr Drug Deliv*. 2017;15(5):652–7. <https://doi.org/10.2174/1567201814666170825160617>
  38. Chang M, Stride E, Edirisinghe M. Nano-organized shells and their application in controlled release. *Ther Deliv*. 2011;2(10):1247–57. <https://doi.org/10.4155/tde.11.94>
  39. Boothroyd CB, Moreno MS, Duchamp M, Kovács A, Monge N, Morales GM, et al. Atomic resolution imaging and spectroscopy of barium atoms and functional groups on graphene oxide. *Ultramicroscopy*. 2014;145:66–73. <https://doi.org/10.1016/j.ultramic.2014.03.004>
  40. Jejuriar A, Lawrie GA, Martin DJ, Grøndahl L. A novel strategy for preparing mechanically robust ionically cross-linked alginate hydrogels. *Biomed Mater*. 2011;6:025010. <https://doi.org/10.1088/1748-6041/6/2/025010>
  41. Rosales TK, Fabi JP. Pectin-based nanoencapsulation strategy to improve the bioavailability of bioactive compounds. *Int J Biol Macromol*. 2022;229:11–21. <https://doi.org/10.1016/j.jbiomac.2022.12.292>
  42. Evy Alice Abigail M. Biochar-based nanocarriers: fabrication, characterization, and application as 2,4-dichlorophenoxyacetic acid nanoformulation for sustained release. *3 Biotech*. 2019;9:317. <https://doi.org/10.1007/s13205-019-1829-y>
  43. Kyomugasho C, Christiaens S, Shpigelman A, Van Loey AM, Hendrickx ME. FT-IR spectroscopy, a reliable method for routine analysis of the degree of methylesterification of pectin in different fruit- and vegetable-based matrices. *Food Chem*. 2015;176:82–90. <https://doi.org/10.1016/j.foodchem.2014.12.033>
  44. Filippov M, Shkolenko GA, Kohn R. Determination of the esterification degree of the pectin of different origin and composition by the method of infrared spectroscopy. *Chemicke Zvesti*. 1978;32 (2):218–22.
  45. Rodsamran P, Sothornvit R. Microwave heating extraction of pectin from lime peel: characterization and properties compared with the conventional heating method. *Food Chem*. 2019;278:364–72. <https://doi.org/10.1016/j.foodchem.2018.11.067>
  46. Cabaniss SE, McVey IF. Aqueous infrared carboxylate absorbances: aliphatic monocarboxylates. *Spectrochim Acta A Mol Biomol Spectrosc*. 1995;51(13):2385–95. [https://doi.org/10.1016/0584-8539\(95\)01479-9](https://doi.org/10.1016/0584-8539(95)01479-9)
  47. Mitra S, Werling KA, Berquist EJ, Lambrecht DS, Garrett-Roe S. CH mode mixing determines the band shape of the carboxylate symmetric stretch in Apo-EDTA, Ca<sup>2+</sup>-EDTA, and Mg<sup>2+</sup>-EDTA. *J Phys Chem A*. 2021;125(22):4867–81. <https://doi.org/10.1021/acs.jpca.1c03061>
  48. Canteri MH, Renard CM, Le Bourvellec C, Bureau S. ATR-FTIR spectroscopy to determine cell wall composition: application on a large diversity of fruits and vegetables. *Carbohydr Polym*. 2019;212:186–96. <https://doi.org/10.1016/j.carbpol.2019.02.021>
  49. Hansen PE, Vakili M, Kamounah FS, Spanget-Larsen J. NH stretching frequencies of intramolecularly hydrogen-bonded systems: an experimental and theoretical study. *Molecules*. 2021;26(24):7651. <https://doi.org/10.3390/molecules26247651>
  50. Smith B. The big review IV: hydrocarbons. *Spectroscopy*. 2025;40 (1):16–9. <https://doi.org/10.56530/spectroscopy.vt7783b7>
  51. Instanano. FTIR functional group search [Internet]. Instanano; 2025 [cited 2025 Apr 2]. Available from: <https://instanano.com/all/characterization/ftir/ftir-functional-group-search/>
  52. Chen XiaoTing CX, Wang TongXin WT. Preparation and characterization of atrazine-loaded biodegradable PLGA nanospheres. *J Integr Agric*. 2019;18(5):1035–41. [https://doi.org/10.1016/S2095-3119\(19\)62613-4](https://doi.org/10.1016/S2095-3119(19)62613-4)
  53. Sahoo S, Manjaiah K, Datta S, Ahmed Shabeer T, Kumar J. Kinetics of metribuzin release from bentonite-polymer composites in water. *J Environ Sci Health B*. 2014;49(8):591–600. <https://doi.org/10.1080/03601234.2014.911578>
  54. Belmokhtar FZ, Elbahri Z, Elbahri M. Preparation and optimization of agrochemical 2,4-D controlled release microparticles using designs of experiments. *J Mex Chem Soc*. 2018;62(1). <https://doi.org/10.29356/jmcs.v62i1.579>
  55. Grillo R, Rosa A, Fraceto L. Poly( $\epsilon$ -caprolactone) nanocapsules carrying the herbicide atrazine: effect of chitosan-coating agent on physicochemical stability and herbicide release profile. *Int J Environ Sci Technol*. 2014;11(6):1691–700.
  56. Sopeña F, Cabrera A, Maqueda C, Morillo E. Controlled release of the herbicide norflurazon into water from ethylcellulose formulations. *J Agric Food Chem*. 2005;53(9):3540–7. <https://doi.org/10.1021/jf048007d>
  57. Stloukal P, Kucharczyk P, Sedlarik V, Bazant P, Koutny M. Low molecular weight poly(lactic acid) microparticles for controlled release of the herbicide metazachlor: preparation, morphology and

release kinetics. J Agric Food Chem. 2012;60(16):4111–9.

### Additional information

**Peer review:** Publisher thanks Sectional Editor and the other anonymous reviewers for their contribution to the peer review of this work.

**Reprints & permissions information** is available at [https://horizonpublishing.com/journals/index.php/PST/open\\_access\\_policy](https://horizonpublishing.com/journals/index.php/PST/open_access_policy)

**Publisher's Note:** Horizon e-Publishing Group remains neutral with regard to jurisdictional claims in published maps and institutional affiliations.

**Indexing:** Plant Science Today, published by Horizon e-Publishing Group, is covered by Scopus, Web of Science, BIOSIS Previews, Clarivate Analytics, NAAS, UGC Care, etc  
See <https://horizonpublishing.com/journals/index.php/PST/>

### indexing\_abstracting

**Copyright:** © The Author(s). This is an open-access article distributed under the terms of the Creative Commons Attribution License, which permits unrestricted use, distribution and reproduction in any medium, provided the original author and source are credited (<https://creativecommons.org/licenses/by/4.0/>)

**Publisher information:** Plant Science Today is published by HORIZON e-Publishing Group with support from Empirion Publishers Private Limited, Thiruvananthapuram, India.